Kinetic Parameters Estimation in a MTR Research and Production Reactor in Subcritical States

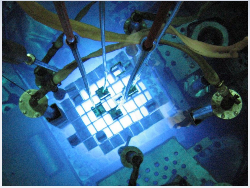

P.A. Bellino A. Gomez G. Estryk C. Grant

National Atomic Energy Commission, Department of Nuclear Energy, Argentina

International Conference on Research Reactors:
Safe Management and Effective Utilization

14-18 November 2011, Rabat, Morocco

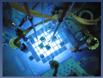

Objectives

Kinetic parameters estimation

- Inverse kinetics as a reactimeter in subcritical states (monitoring a refueling operation).
- Determination of the strength of the neutron source (point kinetic model).
- Characterization of the neutron source. Photoneutron effectiveness estimation (γ^{ph}).
- Neutron noise technique in presence of ^{135}Xe and high gamma exposure rate ($10^6\ R/h$).
- Reactivity and power estimations ($30\ mW$ to $200\ mW$).

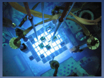

Objectives

Kinetic parameters estimation

- Inverse kinetics as a reactimeter in subcritical states (monitoring a refueling operation).
- Determination of the strength of the neutron source (point kinetic model).
- Characterization of the neutron source. Photoneutron effectiveness estimation (γ^{ph}).
- Neutron noise technique in presence of ^{135}Xe and high gamma exposure rate ($10^6\ R/h$).
- Reactivity and power estimations ($30\ mW$ to $200\ mW$).

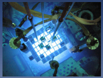

Objectives

Kinetic parameters estimation

- Inverse kinetics as a reactimeter in subcritical states (monitoring a refueling operation).
- Determination of the strength of the neutron source (point kinetic model).
- Characterization of the neutron source. Photoneutron effectiveness estimation (γ^{ph}).
- Neutron noise technique in presence of ^{135}Xe and high gamma exposure rate (10^6 R/h).
- Reactivity and power estimations ($30\,mW$ to $200\,mW$).

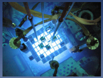

Objectives

Kinetic parameters estimation

- Inverse kinetics as a reactimeter in subcritical states (monitoring a refueling operation).
- Determination of the strength of the neutron source (point kinetic model).
- Characterization of the neutron source. Photoneutron effectiveness estimation (γ^{ph}).
- Neutron noise technique in presence of ^{135}Xe and high gamma exposure rate ($10^6\ R/h$).
- Reactivity and power estimations ($30\ mW$ to $200\ mW$).

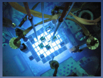

Objectives

Kinetic parameters estimation

- Inverse kinetics as a reactimeter in subcritical states (monitoring a refueling operation).
- Determination of the strength of the neutron source (point kinetic model).
- Characterization of the neutron source. Photoneutron effectiveness estimation (γ^{ph}).
- Neutron noise technique in presence of ^{135}Xe and high gamma exposure rate (10^6 R/h).
- Reactivity and power estimations (30 mW to 200 mW).

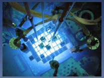

Objectives

Kinetic parameters estimation

- Inverse kinetics as a reactimeter in subcritical states (monitoring a refueling operation).
- Determination of the strength of the neutron source (point kinetic model).
- Characterization of the neutron source. Photoneutron effectiveness estimation (γ^{ph}).
- Neutron noise technique in presence of ^{135}Xe and high gamma exposure rate ($10^6\ R/h$).
- Reactivity and power estimations ($30\,mW$ to $200\,mW$).

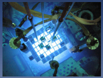

Neutron source

Photoneutrons

- Produced in the reaction $D(\gamma, n)H$ for $E_\gamma > 2{,}23\,MeV$
- Treated as nine extra groups of delayed neutrons in the point kinetic equations.
- Assumed to come from precursors originated during the normal operation of the reactor at full power.
- Measurements were made 36 h after the reactor shutdown. The photoneutron source was assumed to be constant during each measurement ($\sim h$).

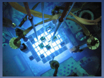

Neutron source

Photoneutrons

- Produced in the reaction $D(\gamma, n)H$ for $E_\gamma > 2{,}23\,MeV$
- Treated as nine extra groups of delayed neutrons in the point kinetic equations.
- Assumed to come from precursors originated during the normal operation of the reactor at full power.
- Measurements were made 36 h after the reactor shutdown. The photoneutron source was assumed to be constant during each measurement ($\sim h$).

Neutron source

Photoneutrons

- Produced in the reaction $D(\gamma, n)H$ for $E_\gamma > 2{,}23\, MeV$
- Treated as nine extra groups of delayed neutrons in the point kinetic equations.
- Assumed to come from precursors originated during the normal operation of the reactor at full power.
- Measurements were made 36 h after the reactor shutdown. The photoneutron source was assumed to be constant during each measurement ($\sim h$).

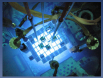

Neutron source

Photoneutrons

- Produced in the reaction $D(\gamma, n)H$ for $E_\gamma > 2{,}23\,MeV$
- Treated as nine extra groups of delayed neutrons in the point kinetic equations.
- Assumed to come from precursors originated during the normal operation of the reactor at full power.
- Measurements were made 36 h after the reactor shutdown. The photoneutron source was assumed to be constant during each measurement ($\sim h$).

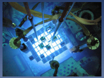

RA-3 core configuration

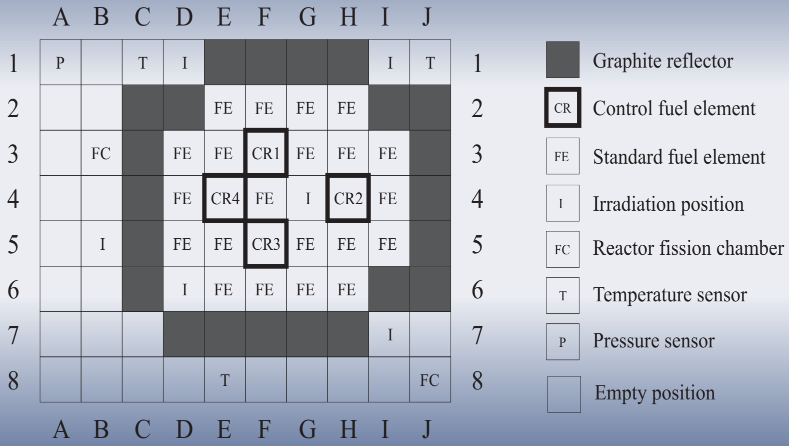

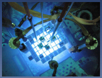

Neutron noise technique

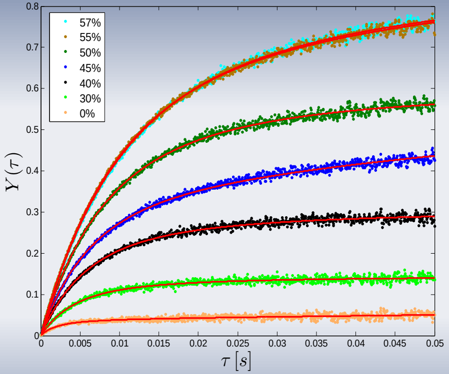

α-Feynman method

$$Y(\tau) = \frac{\epsilon D}{\alpha^2 \Lambda^2}\left(1 - \frac{1 - e^{-\alpha\tau}}{\alpha\tau}\right)$$

D: Diven factor
Λ: Neutron generation time
ϵ: Absolute efficiency ($\sim$ Power)
α: Prompt neutron decay constant

Reactivities: $-6 < \$ < -0{,}5$
Count rate: $1\,10^5\,cps < R < 7\,10^5\,cps$

Power and reactivity are estimated in each stationary subcritical state.

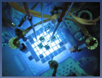

Neutron noise technique

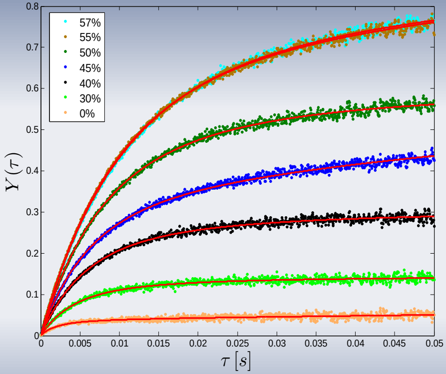

α-Feynman method

$$Y(\tau) = \frac{\epsilon D}{\alpha^2 \Lambda^2}\left(1 - \frac{1 - e^{-\alpha\tau}}{\alpha\tau}\right)$$

D: Diven factor

Λ: Neutron generation time

ϵ: Absolute efficiency ($\sim$ Power)

α: Prompt neutron decay constant

Reactivities: $-6 < \$ < -0{,}5$

Count rate: $1\,10^5 cps < R < 7\,10^5 cps$

Power and reactivity are estimated in each stationary subcritical state.

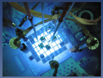

Neutron noise technique

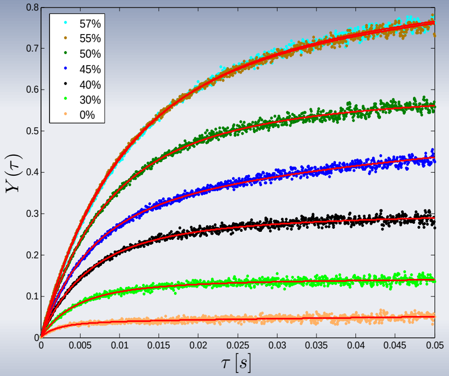

Reactivities: $-6 < \$ < -0{,}5$

Count rate: $1\,10^5 cps < R < 7\,10^5 cps$

α-Feynman method

$$Y(\tau) = \frac{\epsilon D}{\alpha^2 \Lambda^2}\left(1 - \frac{1 - e^{-\alpha\tau}}{\alpha\tau}\right)$$

D: Diven factor

Λ: Neutron generation time

ϵ: Absolute efficiency ($\sim$ Power)

α: Prompt neutron decay constant

Power and reactivity are estimated in each stationary subcritical state.

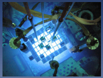

Estimation of α_c

At each subcritical state:

$$\alpha = \alpha_c + \frac{\tilde{S}}{R}$$

By measuring α and R at different subcritical states a linear fit can be performed to obtain α_c.

$$\alpha_c = (106 \pm 1)s^{-1}$$

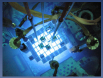

Estimation of α_c

At each subcritical state:

$$\alpha = \alpha_c + \frac{\tilde{S}}{R}$$

By measuring α and R at different subcritical states a linear fit can be performed to obtain α_c.

$$\alpha_c = (106 \pm 1)s^{-1}$$

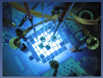

Estimation of α_c

At each subcritical state:

$$\alpha = \alpha_c + \frac{\tilde{S}}{R}$$

By measuring α and R at different subcritical states a linear fit can be performed to obtain α_c.

$$\alpha_c = (106 \pm 1)s^{-1}$$

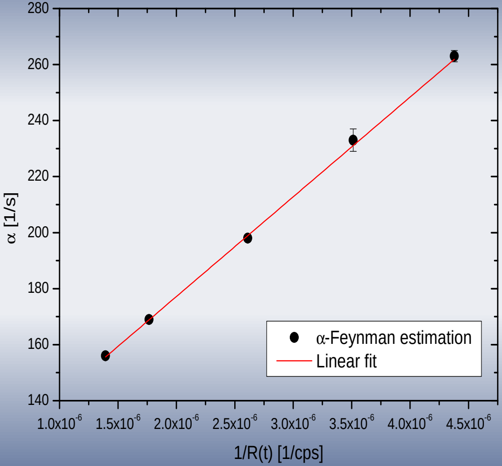

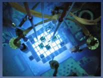

Estimation of γ^{ph}

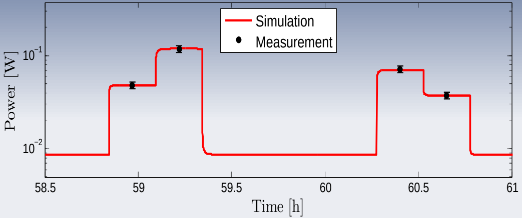

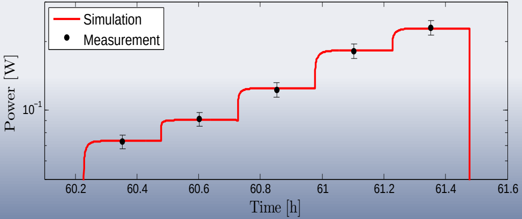

Parametric variation of γ^{ph} in the point kinetics equations until the best fit of the simulation to the measured power is found.

Results

$$\gamma^{ph} = (1{,}15 \pm 0{,}06)\, 10^{-4}$$
$$\gamma^{ph} = (1{,}08 \pm 0{,}06)\, 10^{-4}$$

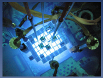

Estimation of γ^{ph}

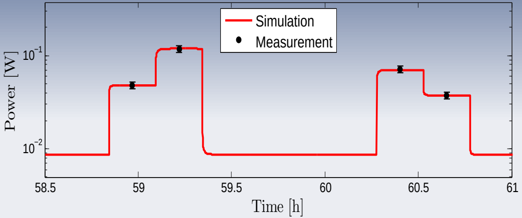

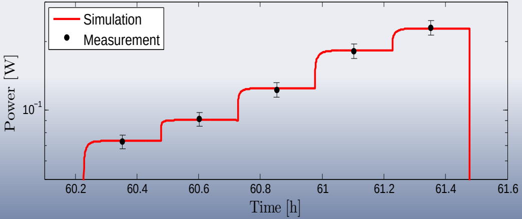

Parametric variation of γ^{ph} in the point kinetics equations until the best fit of the simulation to the measured power is found.

Results

$$\gamma^{ph} = (1{,}15 \pm 0{,}06)\, 10^{-4}$$
$$\gamma^{ph} = (1{,}08 \pm 0{,}06)\, 10^{-4}$$

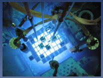

Least square inverse kinetics method

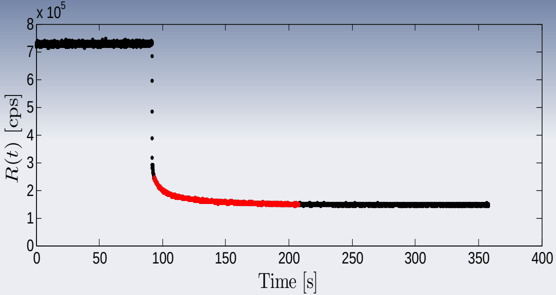

Rod-drop between two subcritical states.

Transient evolution is fitted with a linearized model (LSIKM).

$$R(t) = \frac{\Lambda^*}{\$_f - 1}\tilde{Q}(t) - \frac{\Lambda^*\tilde{S}}{\$_f - 1}$$

Measuring $R(t)$ and $\tilde{Q}(t)$ one can obtain the final state reactivity ($\$_f$) and the source strength ($\tilde{S}$).

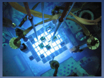

Least square inverse kinetics method

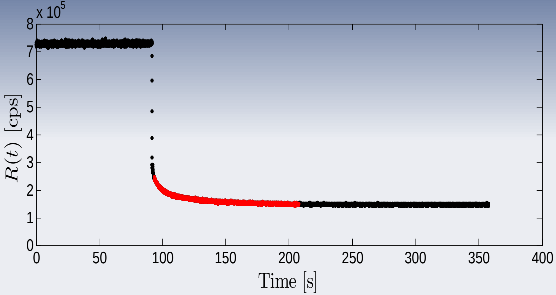

Rod-drop between two subcritical states.

Transient evolution is fitted with a linearized model (LSIKM).

$$R(t) = \frac{\Lambda^*}{\$_f - 1}\tilde{Q}(t) - \frac{\Lambda^* \tilde{S}}{\$_f - 1}$$

Measuring $R(t)$ and $\tilde{Q}(t)$ one can obtain the final state reactivity ($\$_f$) and the source strength ($\tilde{S}$).

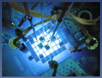

Least square inverse kinetics method

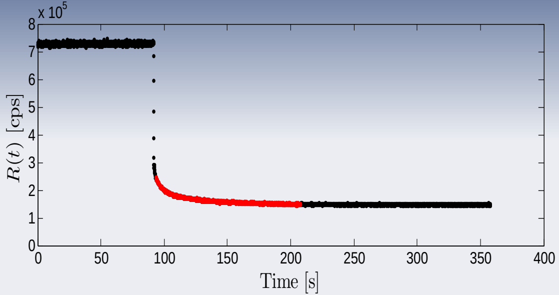

Rod-drop between two subcritical states.

Transient evolution is fitted with a linearized model (LSIKM).

$$R(t) = \frac{\Lambda^*}{\$_f - 1}\tilde{Q}(t) - \frac{\Lambda^* \tilde{S}}{\$_f - 1}$$

Measuring $R(t)$ and $\tilde{Q}(t)$ one can obtain the final state reactivity ($\$_f$) and the source strength ($\tilde{S}$).

Least square inverse kinetics method

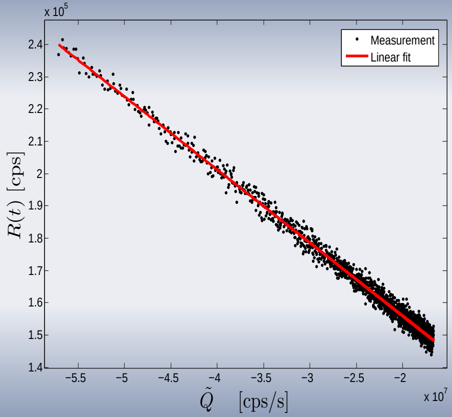

Estimated values

- Detector at G8

$$\tilde{S} = (6{,}90 \pm 0{,}04)\, 10^6 \; cps/s$$

- Detector at B1

$$\tilde{S} = (2{,}6 \pm 0{,}1)\, 10^6 \; cps/s$$

$\tilde{S}$ depends on the detector efficiency
However,it is the magnitude that appears in the inverse kinetics.

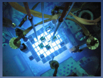

Least square inverse kinetics method

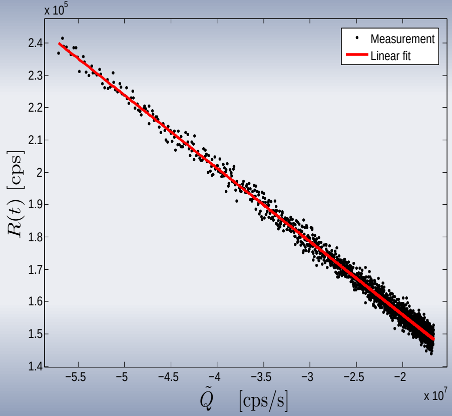

Estimated values

- Detector at G8

$$\tilde{S} = (6{,}90 \pm 0{,}04)\, 10^6 \; cps/s$$

- Detector at B1

$$\tilde{S} = (2{,}6 \pm 0{,}1)\, 10^6 \; cps/s$$

$\tilde{S}$ depends on the detector efficiency

However,it is the magnitude that appears in the inverse kinetics.

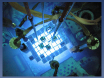

Least square inverse kinetics method

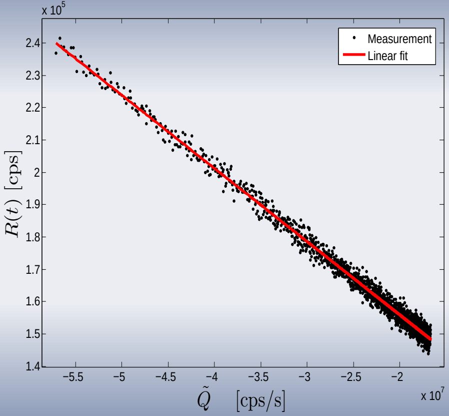

Estimated values

- Detector at G8

$$\tilde{S} = (6{,}90 \pm 0{,}04)\,10^6\ cps/s$$

- Detector at B1

$$\tilde{S} = (2{,}6 \pm 0{,}1)\,10^6\ cps/s$$

$\tilde{S}$ depends on the detector efficiency

However,it is the magnitude that appears in the inverse kinetics.

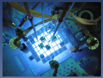

Least square inverse kinetics method

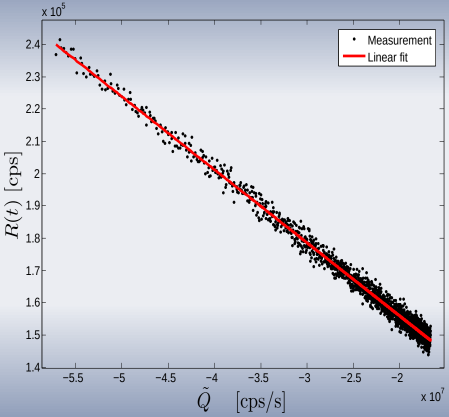

Estimated values

- Detector at G8

$$\tilde{S} = (6{,}90 \pm 0{,}04)\, 10^6 \; cps/s$$

- Detector at B1

$$\tilde{S} = (2{,}6 \pm 0{,}1)\, 10^6 \; cps/s$$

$\tilde{S}$ depends on the detector efficiency

However,it is the magnitude that appears in the inverse kinetics.

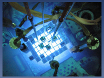

Least square inverse kinetics method

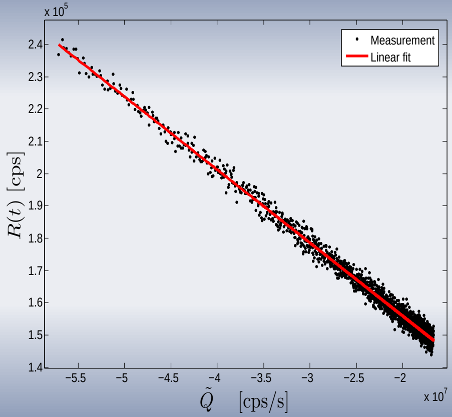

Estimated values

- Detector at G8

$$\tilde{S} = (6{,}90 \pm 0{,}04)\, 10^6\, cps/s$$

- Detector at B1

$$\tilde{S} = (2{,}6 \pm 0{,}1)\, 10^6\, cps/s$$

$\tilde{S}$ depends on the detector efficiency. However,it is the magnitude that appears in the inverse kinetics.

Subcritical reactimeter

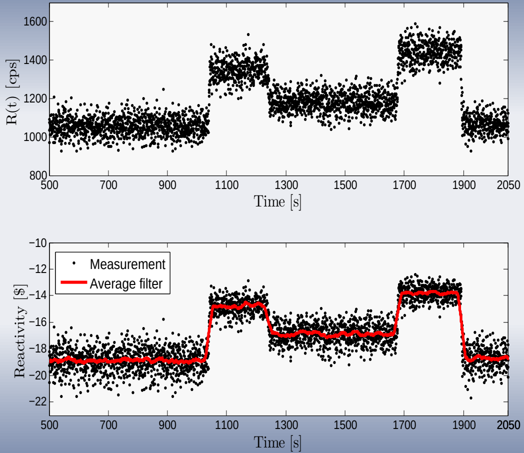

With the estimation of $\tilde{S}$, the reactivity can be obtained measuring the count rate during a refueling operation.

Refueling operation

- Extraction CR from F5
- Extraction FE from F5
- Entering fresh FE at F5
- Entering CR at F5

Subcritical reactimeter

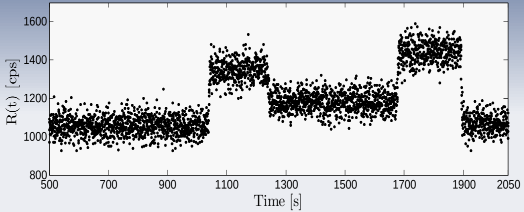

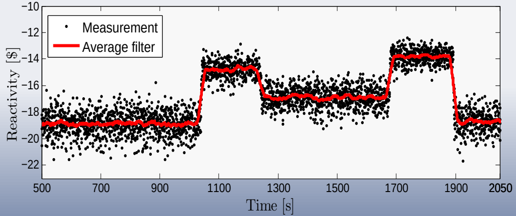

With the estimation of $\tilde{S}$, the reactivity can be obtained measuring the count rate during a refueling operation.

Refueling operation

- Extraction CR from F5
- Extraction FE from F5
- Entering fresh FE at F5
- Entering CR at F5

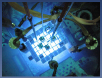

Subcritical reactimeter

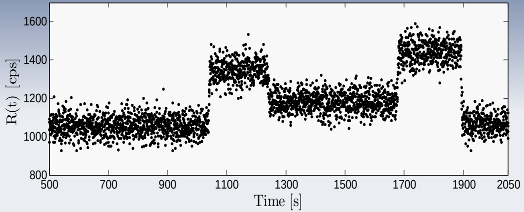

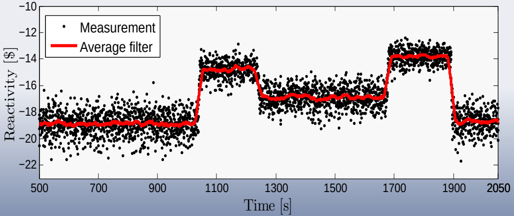

With the estimation of $\tilde{S}$, the reactivity can be obtained measuring the count rate during a refueling operation.

Refueling operation

- Extraction CR from F5
- Extraction FE from F5
- Entering fresh FE at F5
- Entering CR at F5

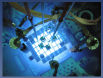

Subcritical reactimeter

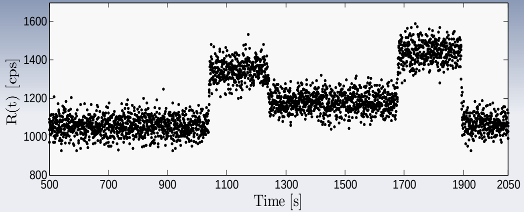

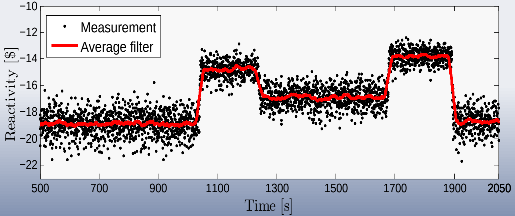

With the estimation of $\tilde{S}$, the reactivity can be obtained measuring the count rate during a refueling operation.

Refueling operation

- Extraction CR from F5
- Extraction FE from F5
- Entering fresh FE at F5
- Entering CR at F5

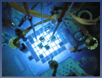

Subcritical reactimeter

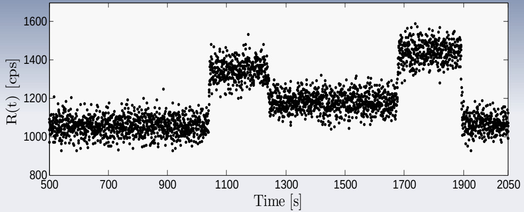

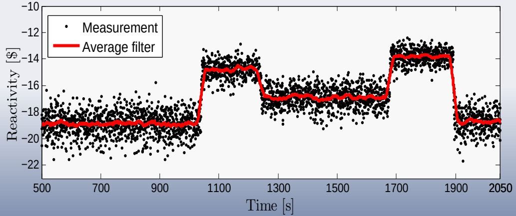

With the estimation of $\tilde{S}$, the reactivity can be obtained measuring the count rate during a refueling operation.

Refueling operation

- Extraction CR from F5
- Extraction FE from F5
- Entering fresh FE at F5
- Entering CR at F5

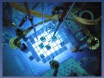

Subcritical reactimeter

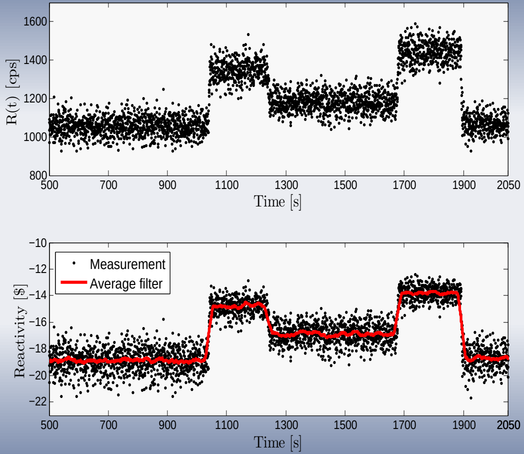

With the estimation of $\tilde{S}$, the reactivity can be obtained measuring the count rate during a refueling operation.

Refueling operation

- Extraction CR from F5
- Extraction FE from F5
- Entering fresh FE at F5
- Entering CR at F5

Subcritical reactimeter

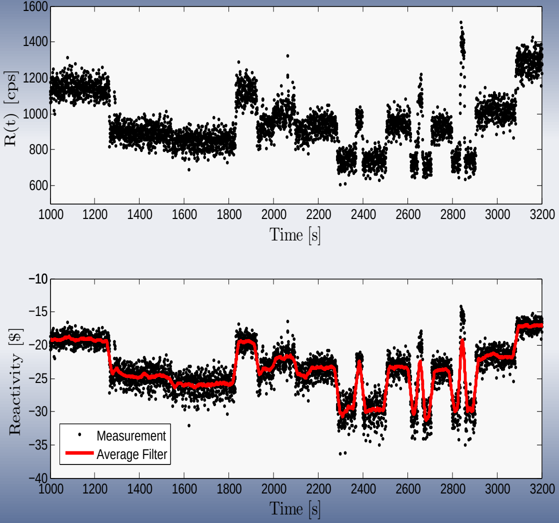

Core 212 to 213

Extraction of burned FE, rotation and entering fresh FE

At these highly subcritical levels, spatial effects become important in reactivity estimations.

Subcritical reactimeter

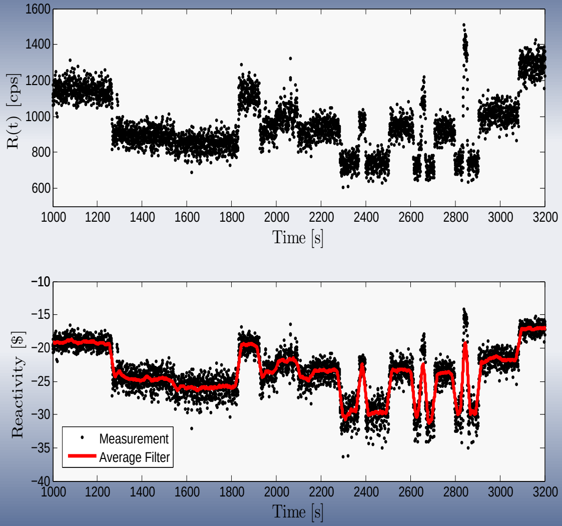

Core 212 to 213

Extraction of burned FE, rotation and entering fresh FE

At these highly subcritical levels, spatial effects become important in reactivity estimations.

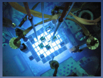

Approach to critical

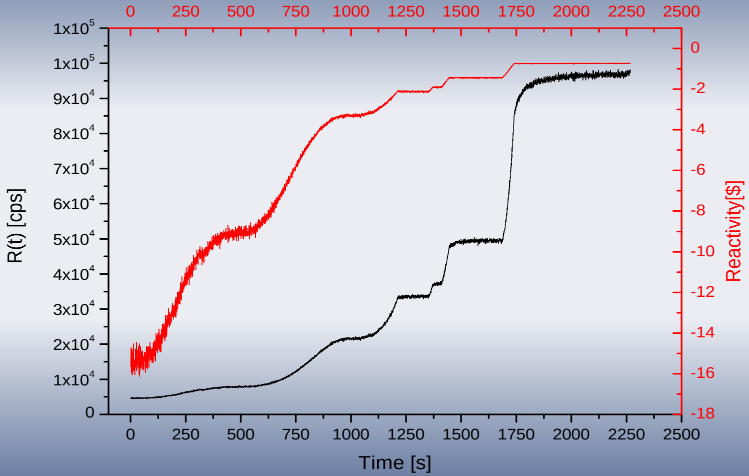

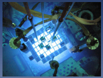

Numerical model

Diffusive code PUMA

Using a homogeneous neutron source in all the fuel channels (First step)

- As the magnitude of the neutron source was not known in advance, all the comparisons were made relative to the first state.
- A refueling operation was calculated.

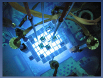

Numerical model

Diffusive code PUMA

Using a homogeneous neutron source in all the fuel channels
(First step)

- As the magnitude of the neutron source was not known in advance, all the comparisons were made relative to the first state.
- A refueling operation was calculated.

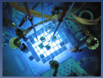

Numerical model

Diffusive code PUMA

Using a homogeneous neutron source in all the fuel channels (First step)

- As the magnitude of the neutron source was not known in advance, all the comparisons were made relative to the first state.
- A refueling operation was calculated.

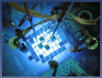

Results from core 212 to 213

Core configuration	i	Experimental		PUMA		
		R_i/R_0	ρ_0/ρ_i	ϕ_i/ϕ_0	P_i/P_0	ρ_0/ρ_i
Core 212	**0**	1	1	1	1	1
	1	0.78 (3)	0.8 (1)	0.784	0.910	0.928
	2	0.74 (3)	0.7 (1)	0.740	0.788	0.809
	3	0.98 (4)	1.00 (5)	0.962	0.878	0.885
	4	0.82 (3)	0.8 (1)	0.806	0.915	0.939
	5	0.81 (3)	0.8 (1)	0.787	0.884	0.901
	6	0.88 (4)	0.9 (1)	0.821	0.783	0.787
Core 213	**7**	1.11 (4)	1.12 (5)	1.113	1.090	1.081

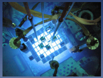

Numerical model

Future improvements

- Calculate the photoneutron source.
- ORIGEN with the information of each FE.
- MCNPX to obtain the photoneutron source.
- MCNPX/PUMA for the neutronic problem.

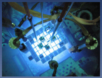

Numerical model

Future improvements

- Calculate the photoneutron source.
- ORIGEN with the information of each FE.
- MCNPX to obtain the photoneutron source.
- MCNPX/PUMA for the neutronic problem.

Numerical model

Future improvements

- Calculate the photoneutron source.
- ORIGEN with the information of each FE.
- MCNPX to obtain the photoneutron source.
- MCNPX/PUMA for the neutronic problem.

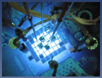

Numerical model

Future improvements

- Calculate the photoneutron source.
- ORIGEN with the information of each FE.
- MCNPX to obtain the photoneutron source.
- MCNPX/PUMA for the neutronic problem.

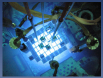

Photoneutron source (MCNPX)

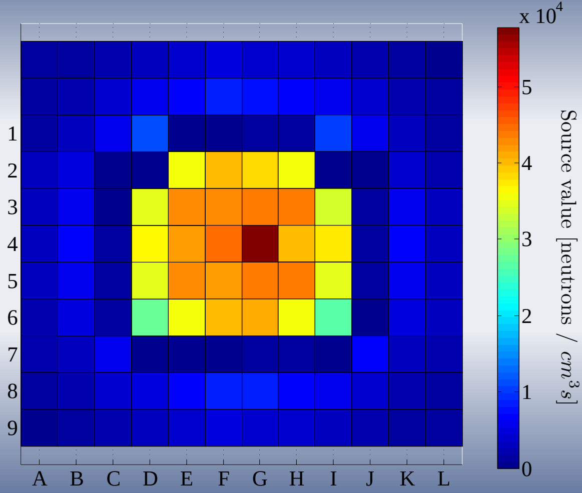

Conclusions

- Measurements at subcritical states with high gamma background and ^{135}Xe.
- With the neutron noise technique reactivities were estimated between -6 and $-0{,}5$ dollars. Power between $30\,mW$ and $200\,mW$.
- First estimations of the pohotoneutron effectiveness $\gamma^{ph} = (1{,}12 \pm 0{,}06)\,10^{-4}$
- Estimation of the source strength value $(\tilde{S})$ that appears in the point kinetics equation.
- Using the inverse kinetics as a subcritical reactimeter
- Monitoring a refueling operation and an approach to critical with a subcritical reactimeter.
- Future measurements with two or more detectors. Detailed studies of spatial effects (correction factors).

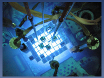

Conclusions

- Measurements at subcritical states with high gamma background and ^{135}Xe.
- With the neutron noise technique reactivities were estimated between -6 and $-0{,}5$ dollars. Power between $30\,mW$ and $200\,mW$.
- First estimations of the pohotoneutron effectiveness $\gamma^{ph} = (1{,}12 \pm 0{,}06)\,10^{-4}$
- Estimation of the source strength value $(\tilde{S})$ that appears in the point kinetics equation.
- Using the inverse kinetics as a subcritical reactimeter
- Monitoring a refueling operation and an approach to critical with a subcritical reactimeter.
- Future measurements with two or more detectors. Detailed studies of spatial effects (correction factors).

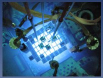

Conclusions

- Measurements at subcritical states with high gamma background and ${}^{135}Xe$.
- With the neutron noise technique reactivities were estimated between -6 and $-0{,}5$ dollars. Power between $30\,mW$ and $200\,mW$.
- First estimations of the pohotoneutron effectiveness $\gamma^{ph} = (1{,}12 \pm 0{,}06)\,10^{-4}$
- Estimation of the source strength value $(\tilde{S})$ that appears in the point kinetics equation.
- Using the inverse kinetics as a subcritical reactimeter
- Monitoring a refueling operation and an approach to critical with a subcritical reactimeter.
- Future measurements with two or more detectors. Detailed studies of spatial effects (correction factors).

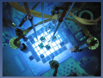

Conclusions

- Measurements at subcritical states with high gamma background and ^{135}Xe.
- With the neutron noise technique reactivities were estimated between -6 and $-0{,}5$ dollars. Power between $30\,mW$ and $200\,mW$.
- First estimations of the pohotoneutron effectiveness $\gamma^{ph} = (1{,}12 \pm 0{,}06)\,10^{-4}$
- Estimation of the source strength value $(\tilde{S})$ that appears in the point kinetics equation.
- Using the inverse kinetics as a subcritical reactimeter
- Monitoring a refueling operation and an approach to critical with a subcritical reactimeter.
- Future measurements with two or more detectors. Detailed studies of spatial effects (correction factors).

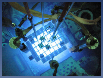

Conclusions

- Measurements at subcritical states with high gamma background and ^{135}Xe.
- With the neutron noise technique reactivities were estimated between -6 and $-0{,}5$ dollars. Power between $30\,mW$ and $200\,mW$.
- First estimations of the pohotoneutron effectiveness $\gamma^{ph} = (1{,}12 \pm 0{,}06)\,10^{-4}$
- Estimation of the source strength value $(\tilde{S})$ that appears in the point kinetics equation.
- Using the inverse kinetics as a subcritical reactimeter
- Monitoring a refueling operation and an approach to critical with a subcritical reactimeter.
- Future measurements with two or more detectors. Detailed studies of spatial effects (correction factors).

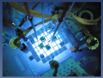

Conclusions

- Measurements at subcritical states with high gamma background and ^{135}Xe.
- With the neutron noise technique reactivities were estimated between -6 and $-0{,}5$ dollars. Power between $30\,mW$ and $200\,mW$.
- First estimations of the pohotoneutron effectiveness $\gamma^{ph} = (1{,}12 \pm 0{,}06)\,10^{-4}$
- Estimation of the source strength value $(\tilde{S})$ that appears in the point kinetics equation.
- Using the inverse kinetics as a subcritical reactimeter
- Monitoring a refueling operation and an approach to critical with a subcritical reactimeter.
- Future measurements with two or more detectors. Detailed studies of spatial effects (correction factors).

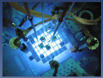

Conclusions

- Measurements at subcritical states with high gamma background and ^{135}Xe.
- With the neutron noise technique reactivities were estimated between -6 and $-0{,}5$ dollars. Power between $30\,mW$ and $200\,mW$.
- First estimations of the pohotoneutron effectiveness $\gamma^{ph} = (1{,}12 \pm 0{,}06)\,10^{-4}$
- Estimation of the source strength value $(\tilde{S})$ that appears in the point kinetics equation.
- Using the inverse kinetics as a subcritical reactimeter
- Monitoring a refueling operation and an approach to critical with a subcritical reactimeter.
- Future measurements with two or more detectors. Detailed studies of spatial effects (correction factors).

Thank you for your attention